

Heavy reflux PSA cycles for CO₂ recovery from flue gas: Part I. Performance evaluation

Steven P. Reynolds · Amal Mehrotra · Armin D. Ebner ·
James A. Ritter

Received: 30 April 2007 / Revised: 3 January 2008 / Accepted: 16 January 2008 / Published online: 31 January 2008
© Springer Science+Business Media, LLC 2008

Abstract This study evaluated nine stripping PSA cycle configurations, all with a heavy reflux (HR) step, some with a light reflux (LR) step, and some with a recovery (REC) or feed plus recycle (F+R) step, for concentrating CO₂ from stack and flue gas at high temperature (575 K) using a K-promoted HTlc. Under the process conditions studied, the addition of the LR step always resulted in a better process performance; and in all cases, the addition of a REC or F+R step surprisingly did not affect the process performance except at low feed throughputs, where either cycle step resulted in a similar diminished performance. The best cycle based on overall performance was a 5-bed 5-step stripping PSA cycle with LR and HR from countercurrent depressurization (CnD) (98.7% CO₂ purity, 98.7% CO₂ recovery and 5.8 L STP/hr/kg feed throughput). The next best cycle was a 5-bed 5-step stripping PSA cycle with LR and HR from LR purge (96.5% CO₂ purity, 71.1% CO₂ recovery and 57.6 L STP/hr/kg feed throughput). These improved performances were caused mainly by the use of a very small purge to feed ratio ($\gamma = 0.02$) for the former cycle and a larger one ($\gamma = 0.50$) for the latter cycle. The former cycle was good for producing CO₂ at high purities and recoveries but at lower feed throughputs, and the latter cycle was useful for obtaining CO₂ at high purities and feed throughputs but at lower recoveries. The best performance of a 4-bed 4-step stripping PSA cycle with HR from CnD was disappointing because of low CO₂ recoveries (99.2% CO₂ purity, 15.2% CO₂ recovery and 72.0 L STP/hr/kg feed throughput). This last result revealed that the recoveries of this cycle

would always be much lower than the corresponding cycles with a LR step, no matter the process conditions, and that the LR step was very important to the performance of these HR cycles for this application and process conditions studied.

Keywords Pressure swing adsorption · Dual reflux · Stripping PSA · Rinse step · Recovery step · Feed plus recycle step · Heavy reflux · Light reflux · Carbon dioxide capture · Global warming

1 Introduction

The production and subsequent release of carbon dioxide into the atmosphere, no matter the source, is becoming an increasingly serious issue with respect to its affect on global warming (White et al. 2003). As one of the more familiar greenhouse gases, carbon dioxide has the ability to warm the planet by trapping energy radiated from the surface of the earth that would otherwise be released to space. One of the major sources of carbon dioxide release into the atmosphere is through the burning of fossil fuels for energy, which unfortunately makes it ubiquitous.

A considerable effort is underway worldwide to curb CO₂ emissions from coal fired and other fossil fuel based power plants, because these plants are responsible for over 40% of the carbon dioxide emissions in the USA alone (Ebner and Ritter 2007). The goal is to capture CO₂ from stack or flue gas, concentrate it to around 90 to 95 vol%, and sequester it somewhere in the Earth. Viable CO₂ capture options include absorption, cryogenic condensation, adsorption, and membrane technologies. To date, however, none of these technologies is economically feasible; so, considerable

S.P. Reynolds · A. Mehrotra · A.D. Ebner · J.A. Ritter (✉)
Department of Chemical Engineering, Swearingen Engineering
Center, University of South Carolina, Columbia, SC 29208, USA
e-mail: ritter@engr.sc.edu

research is being done with all four unit operations in search of a more economically feasible process.

A comprehensive review of the current state of the art on CO₂ capture technologies has been given by Ebner and Ritter (2007), with a focus on adsorption and membrane technologies in this role. They and also Reynolds et al. (2006a) show that a variety of PSA cycles and commercial adsorbents have been studied and even commercialized for concentrating CO₂ from stack or flue gas. However, no consistent reasoning has ever been offered as to why a particular PSA cycle was selected.

In a series of simulation studies, Ritter and co-workers (Reynolds et al. 2005, 2006a, 2006b) have been trying to shed some light on this situation by systematically comparing the performances from increasingly more complex and diverse PSA cycles that have been touted in the literature for CO₂ capture and concentration. Their work on exploiting the use of a high temperature CO₂ adsorbent, namely K-promoted hydrotalcite (HTlc), for recovering CO₂ from stack or flue gas at elevated temperatures, has been fundamental in the sense that the PSA cycles have been compared to each other in a very controlled fashion based simply on linear driving force mass transfer effects and a temperature dependent Langmuir adsorption isotherm (Ding and Alpay 2000, 2001). Therefore, the objective of this work is to expound of those previous studies by evaluating nine stripping PSA cycle configurations, all with a heavy reflux (HR) step, some with a light reflux (LR) step, and some with a recovery (REC) or feed plus recycle (F+R) step, for concentrating CO₂. This present work perhaps represents the most comprehensive comparison to date of a wide range of PSA cycles for CO₂ capture and concentration.

In the three previous studies of stripping PSA cycles for concentrating CO₂ from stack or flue gas at high temperature using a K-promoted HTlc (Reynolds et al. 2005, 2006a, 2006b), literally thousands of simulations were carried out to determine the cycle that resulted in the highest CO₂ purity, recovery and feed throughput. In the first two studies (Reynolds et al. 2005, 2006a), six stripping PSA cycles were evaluated. The three stripping PSA cycles that utilized a heavy reflux (HR) step consistently outperformed the other three cycles that did not utilize this step. These three HR cycles were a 5-bed 5-step stripping PSA cycle with light reflux (LR) and HR from countercurrent depressurization (CnD), a 5-bed 5-step stripping PSA cycle with light reflux (LR) and HR from LR purge, and a 4-bed 4-step stripping PSA cycle with HR from CnD.

In the third study (Reynolds et al. 2006b), the two best performing HR cycles (i.e., the second and third cycles mentioned above) based on CO₂ purity were chosen to study the effects of the adsorption (k_a) and desorption (k_d) mass transfer coefficients of CO₂ in the K-promoted HTlc, since the values reported in the literature varied widely (Ding and Alpay 2000, 2001; Hufton et al. 1999; Soares et al. 2004) and

since those used in the initial work (Reynolds et al. 2005), as adopted from the literature (Ding and Alpay 2001), were quite small. Indeed, the mass transfer effects were very important to the process performance. Simply making k_a and k_d five times greater than the values used in the previous two studies (Reynolds et al. 2005, 2006a), resulted in a CO₂ purity of nearly 90% at a high CO₂ recovery of 85.0% and a reasonable feed throughput of 57.6 L STP/hr/kg. This was the first time, based on the simulation results of the various stripping PSA cycles with a HR step, that a CO₂ purity of nearly 90% was achieved. More importantly, recent work by Ritter and co-workers (Ebner et al. 2006, 2007) showed that the five times greater k_a and k_d were consistent with their experimental and modeling results of the dynamic behavior of CO₂ in a K-promoted HTlc.

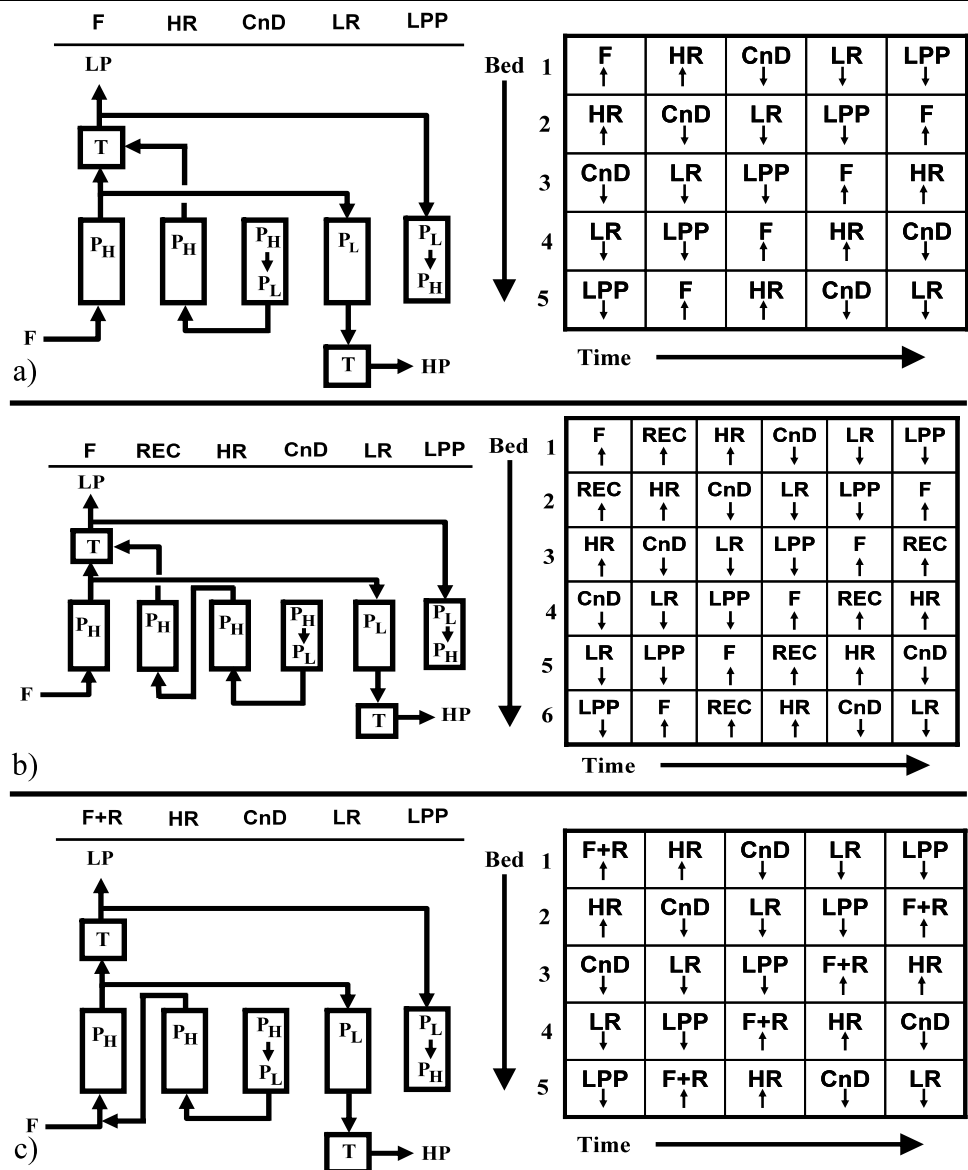
With those results (Ebner et al. 2006, 2007) validating the use of the five times higher k_a and k_d in the simulations, two questions needed to be answered. Were there any other stripping PSA cycles with a HR step that had the potential to further improve the process performance? Were there any process conditions that had not been studied that had the potential to further improve the process performance? The goal of this study is to answer these questions.

The first objective is to introduce two additional cycle steps that have been used in the literature with stripping PSA cycles that have a HR step. These cycle steps are called the recovery (Chue et al. 1995) and recycle (Kikkinides et al. 1993) steps. The second objective is to introduce a novel way of operating the LR step in conjunction with a HR cycle. The third objective is to carry out a comprehensive evaluation of the performance of nine uniquely different stripping PSA cycles with HR, i.e., the three HR cycles mentioned above with and without the recovery or recycle step added. Simulations of these nine HR cycles were carried out using an in-house developed cyclic adsorption process simulator. Part I of this work is limited to evaluating the performance of these cycles; Part II of this work is dedicated to providing a detailed explanation of the trends (Mehrotra et al. 2007).

2 Descriptions of the stripping PSA cycles with heavy reflux

The HR concept is not new to PSA cycles; it is commonly referred to as the high pressure rinse step. Ruthven et al. (1994) and Reynolds et al. (2006a) provide a review of some of the HR PSA cycles that have been used for CO₂ concentration and recovery. This HR or high pressure rinse step involves delivering a purge gas, consisting of pure or highly enriched heavy product, to the feed (or heavy) end of the column at high pressure, usually, but not necessarily, at the feed pressure. It is carried out in series following the feed

Fig. 1 Schematics and cycle sequencing of various heavy reflux PSA cycles analyzed for high temperature CO₂ capture and concentration with the CO₂ selective K-promoted HTIc adsorbent: (a) 5-bed 5-step stripping PSA cycle with LR and HR from CnD, (b) 6-bed 6-step stripping PSA cycle with LR, HR from CnD and REC and (c) 5-bed 5-step stripping PSA cycle with LR, HR from CnD and F+R. F = feed; CnD = countercurrent depressurization; LR = light reflux; HR = heavy reflux; LPP = light product pressurization; REC = recovery; R = recycle; P_L = low pressure; P_H = high pressure; LP = light product; HP = heavy product; T = tank



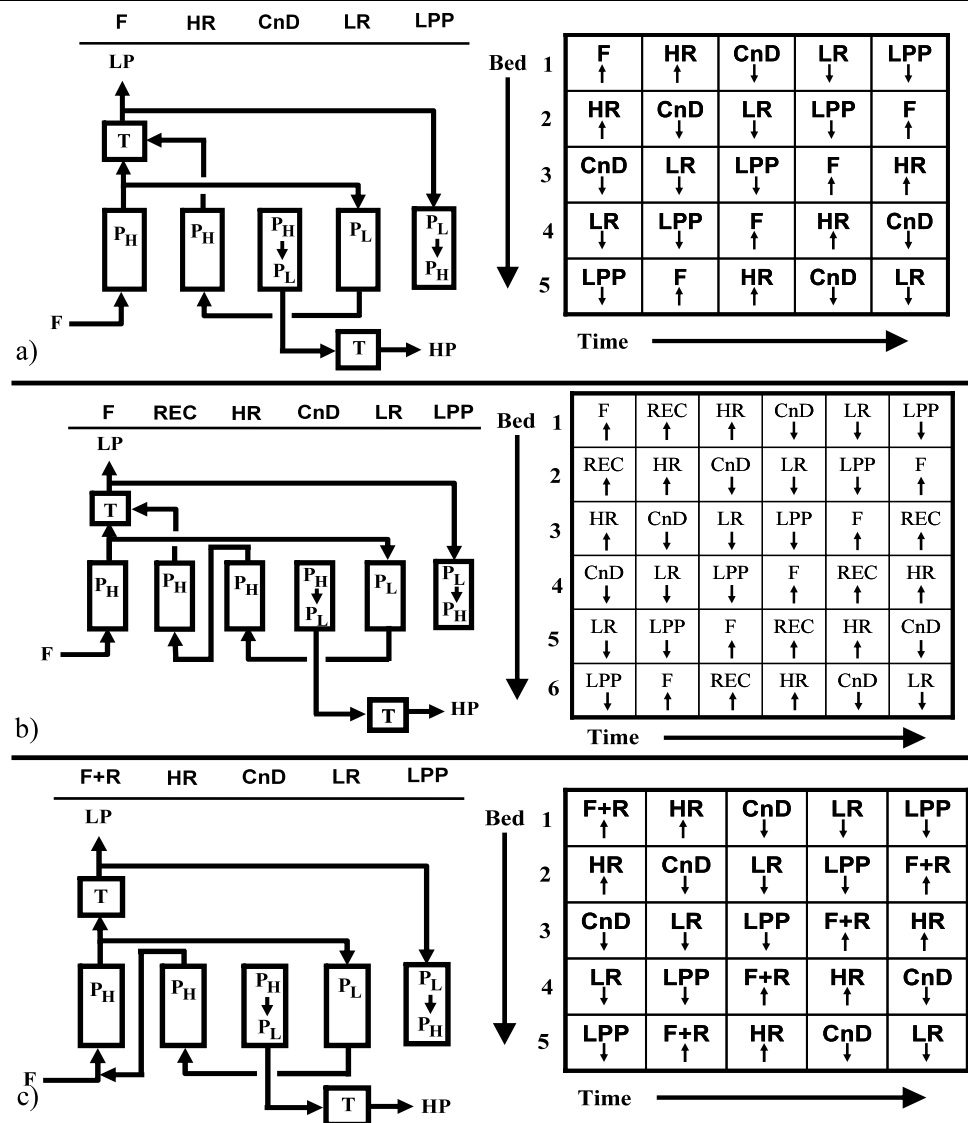
step and used to increase the loading of the heavy component in the column, which, in turn, increases its concentration during the depressurization and/or low pressure purge steps.

However, there are a few different ways to run the HR step in a PSA cycle that depend on the other steps in the cycle. First, the HR gas can be obtained from the depressurization step and/or the low pressure light reflux purge step, depending on whether this latter step is included in the PSA cycle. If it is included, then the PSA cycle is actually a dual plus recycle (F+R) step. The second way is to feed this light reflux cycle with both light and heavy reflux steps.

Second, the light gas effluent coming from the column undergoing the HR step can be managed in several ways. In most cases there are three choices. It can be taken as part

of the light product. But, operating the cycle in this manner may limit the recovery of the heavy component, as some of it can be lost in this light product. Instead, it can also be recycled back into the process for subsequent recovery as heavy product. There are two ways to recycle this light gas effluent back into the process. The first way is to simply blend this light gas effluent with the feed gas during the feed step (Kikkinides et al. 1993). This approach does not add another step to the cycle and is referred to here as the feed plus recycle (F+R) step. The second way is to feed this light gas effluent to the heavy end of another column in between the feed and heavy reflux steps (Chue et al. 1995). This approach adds another step to the cycle and is referred to here as the recovery (REC) step.

Fig. 2 Schematics and cycle sequencing of various heavy reflux PSA cycles analyzed for high temperature CO₂ capture and concentration with the CO₂ selective K-promoted HTlc adsorbent: (a) 5-bed 5-step stripping PSA cycle with LR and HR from LR purge, (b) 6-bed 6-step stripping PSA cycle with LR, HR from LR purge and REC and (c) 5-bed 5-step stripping PSA cycle with LR, HR from LR purge and F+R. F = feed; CnD = countercurrent depressurization; LR = light reflux; HR = heavy reflux; LPP = light product pressurization; REC = recovery; R = recycle; P_L = low pressure; P_H = high pressure; LP = light product; HP = heavy product; T = tank

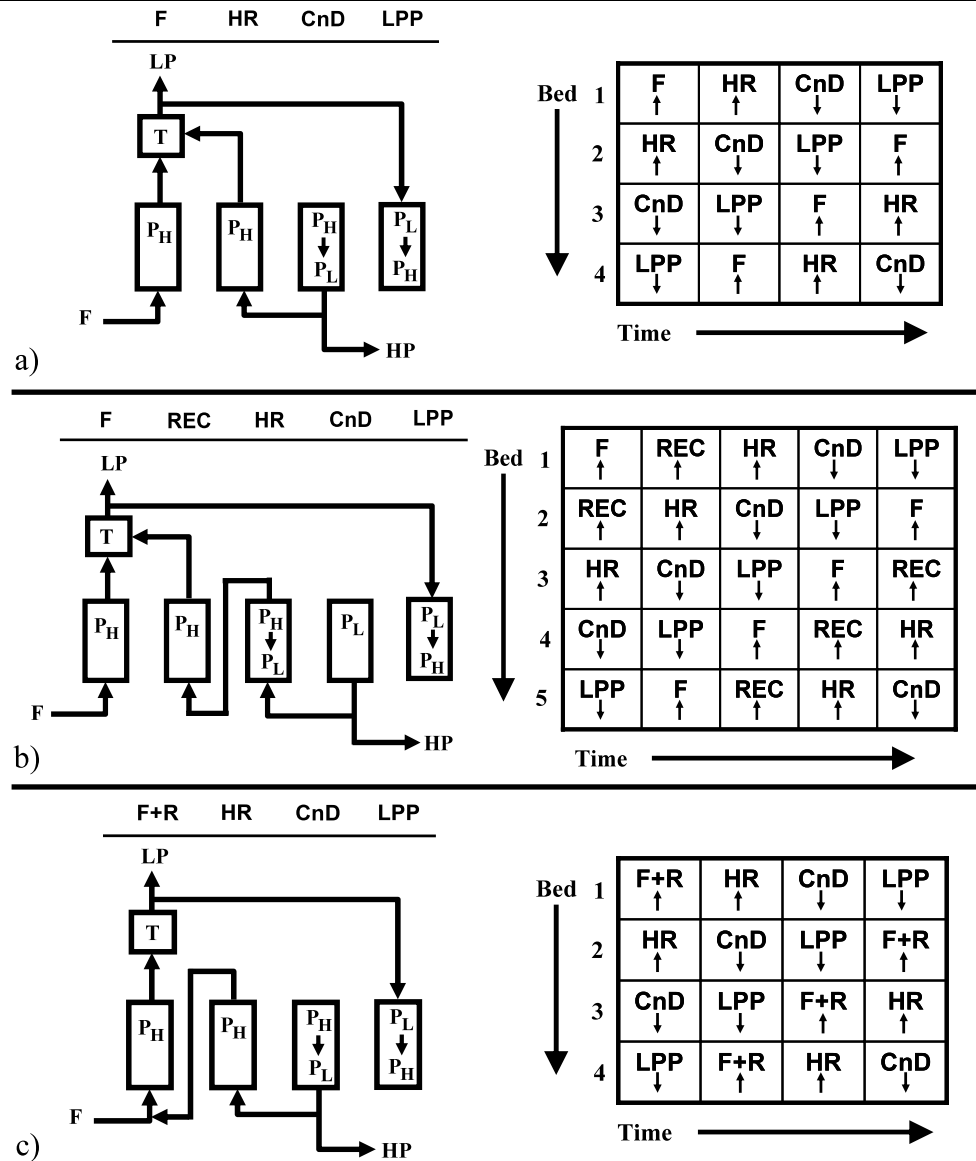


A recovery or recycle step was added to each of the three stripping PSA cycles with HR that were studied previously (Reynolds et al. 2006a, 2006b). In this way, nine different stripping PSA cycles with HR were formulated: a 5-bed 5-step stripping PSA cycle with LR and HR from CnD, alone and with the addition of a REC or F+R step; a 5-bed 5-step stripping PSA cycle with LR and HR from LR purge, alone and with the addition of a REC or F+R step; and a 4-bed 4-step stripping PSA cycle with HR from CnD, alone and with the addition of a REC or F+R step. The schematics and cycle sequencing of these nine stripping PSA cycles with HR are displayed in Figs. 1, 2 and 3, respectively.

The stripping PSA cycle in Fig. 1a contained the following steps: high pressure (P_H) adsorption with feed (F) just above atmospheric pressure, cocurrent high-pressure

adsorption with heavy product purge as heavy reflux (HR), countercurrent depressurization (CnD) from P_H to a lower (vacuum) pressure (P_L), countercurrent low-pressure desorption with light product purge as light reflux (LR), and light product pressurization (LPP) from P_L to P_H . All of the effluent from the CnD step was recompressed to P_H and used as the feed to the column undergoing the HR step. All of the effluent from the LR step was recovered as heavy product. The recovery (REC) step was added to this cycle by taking the light product effluent from the column undergoing the HR step, which was essentially at the feed pressure, and sending it to the column that just finished the feed step, as shown in Fig. 1b. The feed plus recycle (F+R) step was added to this cycle by taking the light product effluent from the column undergoing the HR step, which was essentially at the feed pressure, blending it with feed gas, and sending

Fig. 3 Schematics and cycle sequencing of various heavy reflux PSA cycles analyzed for high temperature CO₂ capture and concentration with the CO₂ selective K-promoted HTlc adsorbent: **(a)** 4-bed 4-step stripping PSA cycle with HR from CnD, **(b)** 5-bed 5-step stripping PSA cycle with HR from CnD and REC and **(c)** 4-bed 4-step stripping PSA cycle with HR from CnD and F+R. F = feed; CnD = countercurrent depressurization; HR = heavy reflux; LPP = light product pressurization; REC = recovery; R = recycle; P_L = low pressure; P_H = high pressure; LP = light product; HP = heavy product



this blended gas to the column undergoing the feed plus recycle step, as shown in Fig. 1c.

The cycles shown in Figs. 2a, 2b and 2c were the same as those in Figs. 1a, 1b and 1c, except for the cycle step that was used to produce the HR gas. In this case, all of the effluent from the LR step (in lieu of the CnD step) was recompressed to P_H and used as the feed to the column undergoing the HR step. All of the effluent from the CnD step (in lieu of the LR step) was recovered as heavy product.

The cycles in Figs. 3a, 3b and 3c were the same as those in Figs. 1a, 1b and 1c, or Figs. 2a, 2b and 2c, except that none of those cycles had a light reflux step. This meant that some specified fraction of the effluent from the CnD step was recompressed to P_H and used as the feed to the column undergoing the HR step. The remaining fraction of the

effluent from the CnD step was recovered as heavy product.

In all cases, the heavy product (mainly CO₂) was enriched and recovered during the CnD or LR step, and the light product (mainly N₂ and H₂O) was recovered during the F, HR, REC and/or F+R steps. The purge or pressurization gases used during the LR or LPP step came directly from the light effluent end of the bed undergoing the F or F+R step. The heavy reflux gas used during the HR step came directly from the heavy effluent end of the bed undergoing either the CnD or LR step. The recovery gas used during the REC step was obtained from the light effluent end of the bed undergoing the HR step. The recycle gas that was blended with the feed and used during the F+R step came from the light effluent end of the bed undergoing the HR

step. In every case these recycled column effluents retained their time-dependent composition and temperature.

The periodic state process performance of these nine PSA cycles was judged by the CO₂ recovery (R), CO₂ purity ($y_{\text{CO}_2,HP}$), and feed throughput (θ). R was defined as the number of moles of CO₂ leaving the bed during the steps where heavy product was withdrawn from the system divided by the number of moles of CO₂ entering the bed in the feed. $y_{\text{CO}_2,HP}$ was defined as the average mole fraction of CO₂ leaving the bed during the steps where heavy product was withdrawn from the system. θ was defined as the total amount of feed fed to the process during one complete cycle divided by the total cycle time and the mass of adsorbent in all the columns.

3 Physical properties

The bed characteristics, gas phase species, and K-promoted HTlc adsorbent transport and thermodynamic properties used in the mathematical model are shown in Table 1. Data (Ding and Alpay 2000, 2001) for CO₂ adsorption on the K-promoted HTlc adsorbent were fitted to a temperature dependent Langmuir isotherm model. This model and the corresponding fit of the data to it are shown elsewhere (Reynolds et al. 2006a). The isosteric heat of adsorption (ΔH_i) was estimated from the temperature dependence of the isotherm parameter b_i .

The linear driving force adsorption and desorption mass transfer coefficients for CO₂ in this K-promoted HTlc were based on values obtained recently by Ritter and co-workers (Ebner et al. 2006, 2007). As mentioned above, the values shown in Table 1 are five times higher than those used in the three previous studies (Reynolds et al. 2005, 2006a, 2006b), which were taken from the work of Ding and Alpay (2001). Five times higher mass transfer coefficients were also used

in some of the simulations of the most recent work by the authors, with very positive effects (Reynolds et al. 2006b).

The other components in the system, namely N₂ and H₂O, were considered to be inert with this adsorbent (Ding and Alpay 2000). Therefore, their adsorption isotherm parameters, mass transfer coefficients and adsorbed phase heat capacities were set to zero. The gas phase properties for N₂ and H₂O, such as their gas phase heat capacities, were accounted for in the model.

The column radius (r_b) and length (L), and the corresponding heat transfer coefficient (h) were adopted from an experimental setup described by Liu et al. (1998). The values are given in Table 1. The reason why these bed dimensions were chosen for this and all previous studies (Reynolds et al. 2005, 2006a, 2006b) was because Liu et al. (1998) actually measured the heat transfer coefficient for a bed with these dimensions. In fact, it is noteworthy that although only simulation results are presented and discussed below, the mathematical model used to obtain these results has been validated against extensive butane-nitrogen-activated carbon PSA experiments carried out by Liu et al. (1999), and CO₂-nitrogen-K-promoted HTlc breakthrough experiments carried out by Ding and Alpay (2001) (results not shown).

4 Mathematical model

The rigorous PSA process simulator utilized in this study was the same as that developed and presented in detail by Reynolds et al. (2006a). It suffices to state that the model accounts for heat and mass transfer effects, velocity variation in the bed, and fully integrates the pressure changing steps. The only changes to that model were the boundary conditions for the REC and F+R steps when used. The initial and boundary conditions affected by the REC step were:

$$\begin{array}{llll} \text{REC:} & \text{at } t = 0: & y_i = y_{i,F}, & T = T_F, & q_i = q_{i,F}, & \text{for all } z \\ & \text{at } z = 0: & y_i = y_{i,HR}(t), & T = T_{HR}(t), & u = u_{REC}, & \text{for all } t \\ \text{HR:} & \text{at } t = 0: & y_i = y_{i,REC}, & T = T_{REC}, & q_i = q_{i,REC}, & \text{for all } z \\ & \text{at } z = 0: & y_i = y_{i,CnD}(t) \text{ or} & T = T_{CnD}(t) \text{ or} & u = u_{REC}, & \text{for all } t \\ & & y_i = y_{i,LR}(t), & T = T_{LR}(t), & & \end{array}$$

The initial and boundary conditions affected by the F+R step were:

$$\begin{array}{llll} \text{F+R:} & \text{at } t = 0: & y_i = y_{i,LPP}, & T = T_{LPP}, & q_i = q_{i,LPP}, & \text{for all } z \\ & \text{at } z = 0: & y_i = y_{i,F+R}(t), & T = T_f, & u = u_{F+R}, & \text{for all } t \\ \text{HR:} & \text{at } t = 0: & y_i = y_{i,REC}, & T = T_{REC}, & q_i = q_{i,REC}, & \text{for all } z \\ & \text{at } z = 0: & y_i = y_{i,CnD}(t) \text{ or} & T = T_{CnD}(t) \text{ or} & u = u_{REC}, & \text{for all } t \\ & & y_i = y_{i,LR}(t), & T = T_{LR}(t), & & \end{array}$$

Table 1 Bed characteristics, gas phase species, and K-promoted HTlc adsorbent transport and thermodynamic properties

<i>Bed, K-promoted HTlc adsorbent, and process characteristics</i>	
Bed length (L)	0.2724 m
Bed radius (r_b)	0.0387 m
Bed porosity (ϵ)	0.48
Adsorbent particle porosity (χ)	0.0
Fraction of χ occupied by adsorbed phase (φ)	0.0
Adsorbent particle density (ρ_p)	1563 kg/m ³
Adsorbent particle heat capacity ($C_{p,p}$)	0.850 kJ/kg/K
CO ₂ -HTlc Isosteric heat of adsorption (ΔH_i)	9.29 kJ/mol
Heat transfer coefficient (h)	0.00067 kW/m ² /K
CO ₂ -HTlc mass transfer coefficient: ads (k_a), des (k_d)	0.029 s ⁻¹ , 0.003 s ⁻¹
Feed mole fractions: CO ₂ , N ₂ , and H ₂ O	0.15, 0.75 and 0.10
Feed (T_f) and wall temperature (T_o)	575 K
High pressure (P_H) (absolute)	139.7 kPa
Low pressure (P_L) (absolute)	11.64 kPa
P_H/P_L	12.0
<i>Adsorption isotherm model and parameters for CO₂ on K-promoted HTlc</i>	
$q^* = \frac{q_1^s b P y}{1 + b P y}$ where $q^s = q_1^s T + q_2^s$ and $b = b^0 \exp(\frac{B^0}{T})$	
q_1^s (mol/kg/K)	-1.5277E-3
q_2^s (mol/kg)	1.7155
b^0 (kPa ⁻¹)	0.0203
B^0 (K)	1118.1
<i>Gas (and adsorbed) phase heat capacity model and coefficients for CO₂, N₂ and H₂O</i>	
$C_{p,g} = \sum_{i=1}^N y_i C_{p,g,i}$ where $C_{p,g,i} = A_i + B_i T + C_i T^2 + D_i T^3$	
A_i for CO ₂ , N ₂ , and H ₂ O (kJ/mol/K)	1.9795E-2, 3.1123E-2, 3.2221E-2
B_i for CO ₂ , N ₂ , and H ₂ O (kJ/mol/K ²)	7.3437E-5, -1.3553E-5, 1.9217E-6
C_i for CO ₂ , N ₂ , and H ₂ O (kJ/mol/K ³)	-5.6019E-8, 2.6772E-8, 1.0548E-8
D_i for CO ₂ , N ₂ , and H ₂ O (kJ/mol/K ⁴)	1.7153E-11, 1.1671E-11, -3.5930E-12

Note that the temperature and gas phase mole fraction boundary conditions for the HR step depended on whether the gas came from the CnD or LR step. Also, $y_{i,F+R}(t)$ is the average, time-dependent concentration obtained by blending the feed with the effluent from the HR step, as given by:

$$y_{i,F+R}(t) = \frac{y_{i,f} \cdot Q_f + y_{i,HR}(t) \cdot Q_{HR}(t)}{Q_f + Q_{HR}(t)} \tag{1}$$

5 Results and discussion

Over three hundred simulations of the nine different stripping PSA cycle configurations with HR were carried out

to the periodic state using the in-house developed cyclic adsorption process simulator. All nine cycle configurations are shown in Figs. 1 to 3. Table 1 shows the bed characteristics, gas phase species, and K-promoted HTlc adsorbent transport and thermodynamic properties. Table 1 also shows the parameters that were held constant in all cases, like the feed and wall temperatures (575 K), and the high to low pressure ratio ($P_H/P_L = 12$). Table 2 indicates the ranges of process conditions studied and corresponding performances achieved in terms of feed throughput, CO₂ purity, and CO₂ recovery for each of the nine PSA cycle configurations. Table 3 provides a summary of the best process performances achieved, based on the highest CO₂ purity obtained for a given PSA cycle configuration and set of corresponding process conditions. Figures 4 to 9 present a sys-

Table 2 Range of process conditions studied and corresponding performances achieved in terms of feed throughput, and CO₂ purity and CO₂ recovery for each of the six stripping PSA cycle configurations

Stripping PSA cycle configuration ^a	Feed throughput (L STP/hr/kg)	Cycle time ^b (s)	Heavy product recycle ratio ^c	CO ₂ purity ^d (%)	CO ₂ recovery ^d (%)
5-bed 5-step cycle with LR and HR from CnD (Fig. 1a)	5.8–57.6	500–2500	1.0	70.8–98.7 (63.5) (98.7) [57.6] [5.8]	26.7–99.9 (96.4) (78.7) [57.6] [5.8]
6-bed 6-step cycle with LR, HR from CnD and REC (Fig. 1b)	4.8–48.0	600–3000	1.0	70.8–98.6 (63.6) (91.3) [48.0] [4.8]	26.7–98.9 (96.4) (78.6) [48.0] [4.8]
5-bed 5-step cycle with LR, HR from CnD and F+R (Fig. 1c)	5.8–57.6	500–2500	1.0	71.0–98.6 (63.1) (91.8) [57.6] [5.8]	26.4–99.5 (96.5) (78.7) [57.6] [5.8]
5-bed 5-step cycle with LR and HR from LR purge (Fig. 2a)	5.8–57.6	500–2500	1.0	25.5–96.6 (98.5) (71.1) [5.8] [57.6]	43.6–99.9 (91.6) (42.2) [57.6] [11.5]
6-bed 6-step cycle with LR, HR from LR purge and REC (Fig. 2b)	4.8–48.0	600–3000	1.0	25.4–96.5 (98.1) (71.1) [4.8] [48.0]	43.6–99.5 (91.6) (42.1) [48.0] [9.6]
5-bed 5-step cycle with LR, HR from LR purge and F+R (Fig. 2c)	5.8–57.6	500–2500	1.0	25.6–96.5 (98.6) (71.0) [5.8] [57.6]	43.6–99.3 (91.6) (52.0) [57.6] [5.8]
4-bed 4-step cycle with HR from CnD (Fig. 3a)	7.2–72.0	400–2000	0.2–0.8	30.3–99.2 (100) (15.0) [7.2] [72.0]	12.6–100 (76.5) (37.1) [72.0] [7.2]
5-bed 5-step cycle with HR from CnD and REC (Fig. 3b)	5.8–57.6	500–2500	0.2–0.8	30.0–99.1 (98.9) (15.0) [5.8] [57.6]	12.4–99.3 (75.8) (30.1) [57.6] [5.8]
4-bed 4-step cycle with HR from CnD and F+R (Fig. 3c)	7.2–72.0	400–2000	0.2–0.8	31.3–99.2 (99.3) (15.2) [7.2] [72.0]	12.5–99.0 (76.4) (30.0) [72.0] [7.2]

^aThe cycle configuration corresponds to the figure number shown in parentheses

^bAll step times t_s were equal in length

^cThe light product purge to feed ratio always ranges from 0.02–0.50

^dThe values in parentheses correspond to the CO₂ recovery achieved for the highest and lowest CO₂ purity (column 5), and the CO₂ purity achieved for the highest and lowest CO₂ recovery (column 6). The values in brackets correspond to the feed throughput (L STP/hr/kg) achieved for the highest and lowest CO₂ purity (column 5), and the feed throughput achieved for the highest and lowest CO₂ recovery (column 6)

tematic account of the performances of these nine stripping PSA cycles with HR in terms of CO₂ purity versus CO₂ recovery plots. However, the discussions below are limited to evaluating only the performance of each HR PSA cycle. Detailed explanations of the observed and sometimes very subtle trends are provided in Part II of this study (Mehrotra et al. 2007).

5.1 Stripping PSA cycles with LR and HR from CnD, with and without a REC or F+R step

The 5-bed 5-step stripping PSA cycle with light reflux (LR) and heavy reflux (HR) from countercurrent depressurization (CnD) consisted of five interconnected beds each undergoing in succession five cycle steps of equal duration, as shown

Table 3 Best performance achieved based on highest CO₂ purity obtained for a given stripping PSA cycle configuration and set of corresponding conditions

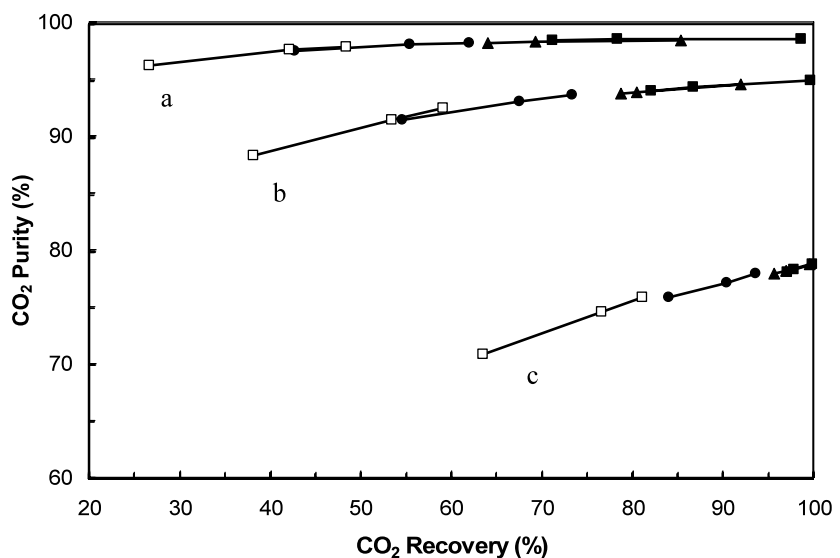
Stripping PSA cycle configuration ^a	Feed throughput (L STP/hr/kg) ^b	Light product purge to feed ratio	Heavy product recycle ratio	Cycle time ^c (s)	CO ₂ purity (%)	CO ₂ recovery (%)
5-bed 5-step cycle with LR and HR from CnD (Fig. 1a)	5.8 (0.5)	0.02	1.0	500	98.7	98.7
6-bed 6-step cycle with LR, HR from CnD and REC (Fig. 1b)	4.8 (0.5)	0.02	1.0	600	98.6	91.3
5-bed 5-step cycle with LR, HR from CnD and F+R (Fig. 1c)	5.8 (0.5)	0.02	1.0	500	98.6	91.8
5-bed 5-step cycle with LR and HR from LR purge (Fig. 2a)	57.6 (5.0)	0.50	1.0	2500	96.6	71.1
6-bed 6-step cycle with LR, HR from LR purge and REC (Fig. 2b)	48.0 (5.0)	0.50	1.0	3000	96.5	71.1
5-bed 5-step cycle with LR, HR from LR purge and F+R (Fig. 2c)	57.6 (5.0)	0.50	1.0	2500	96.5	71.0
4-bed 4-step cycle with HR from CnD (Fig. 3a)	72.0 (5.0)	–	0.8	2000	99.2	15.2
5-bed 5-step cycle with HR from CnD and REC (Fig. 3b)	57.6 (5.0)	–	0.8	2500	99.1	15.0
4-bed 4-step cycle with HR from CnD and F+R (Fig. 3c)	72.0 (5.0)	–	0.8	2000	99.2	15.2

^aThe cycle configuration corresponds to the figure number shown in parentheses

^bValues in parentheses correspond to the feed flow rate Q_F in L STP/min

^cAll step times t_s were equal in length

Fig. 4 Performance curves from the 5-bed 5-step stripping PSA cycle with LR and HR from CnD (Fig. 1a) for $\gamma =$ (a) 0.02, (b) 0.10, and (c) 0.50. Each line corresponds to three runs with t_s increasing from right to left ($t_s = 100, 300,$ and 500 s). Symbols: filled squares— $\theta = 5.8$ ($Q_F = 0.5$); filled triangles— $\theta = 11.5$ ($Q_F = 1.0$); filled circles— $\theta = 34.6$ ($Q_F = 3.0$); empty squares— $\theta = 57.6$ ($Q_F = 5.0$). The performance curves from the corresponding stripping PSA cycle with LR, HR from CnD, and with REC or F+R were essentially the same (not shown)



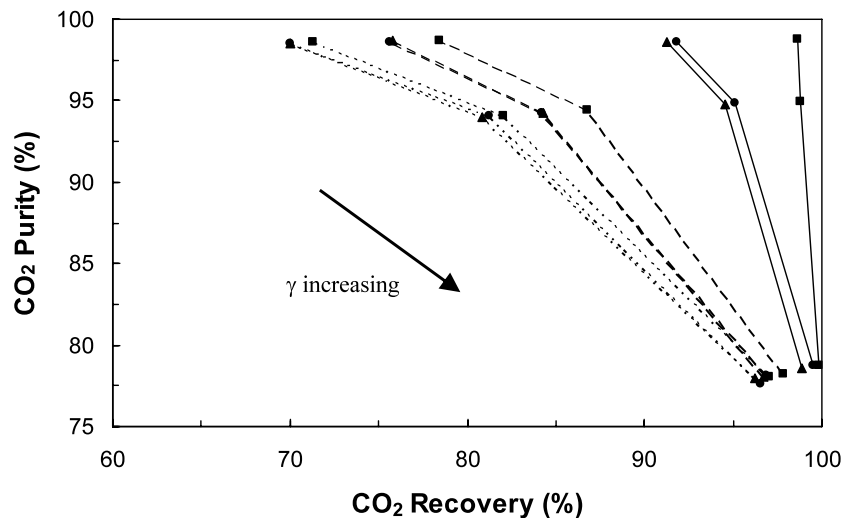


Fig. 5 Performance curves comparing the results from the three stripping PSA cycles with LR and HR from CnD with and without REC or F+R steps and for $Q_F = 0.5$ LSTP/min. Lines: solid— $t_s = 100$ s; dashed— $t_s = 300$ s; dotted— $t_s = 500$ s. Symbols: squares—5-bed 5-step stripping PSA cycle with LR and HR from

CnD ($\theta = 5.8$ LSTP/hr/kg); triangles—6-bed 6-step stripping PSA cycle with LR, HR from CnD and REC ($\theta = 4.8$ LSTP/hr/kg); circles—5-bed 5-step stripping PSA cycle with LR, HR from CnD and F+R ($\theta = 5.8$ LSTP/hr/kg)

in Fig. 1a. The heavy product (CO_2) was recovered only during the LR step, as all of the effluent from the CnD step was recycled to the HR step, i.e., the recycle ratio was equal to one ($R_R = 1.0$) in this case. This mode of operation contrasted with previous studies of this cycle (Reynolds et al. 2006a, 2006b), wherein the heavy product was recovered not only during the LR step, but also during the CnD step with R_R varying from 0.2 to 0.8. In those studies, the CO_2 purity always increased with increasing R_R , which is why $R_R = 1.0$ was always used in this study.

Thirty-six different cases were simulated over the range of parameters listed in Table 2. Three light product purge to feed ratios (γ), three cycle step times (t_s), and four feed throughputs (θ) were investigated. Note that the largest value of γ investigated here of 0.5 was the only value investigated in the previous work (Reynolds et al. 2006a), because it was concluded that the CO_2 purity always increased with decreasing γ . The notion here was to determine if using a very small value of γ , like $\gamma = 0.02$, could further improve the purity. A purge to feed ratio of this magnitude, in conjunction with a HR cycle, has not been discussed in the literature. The effects of γ , t_s , and θ on the process performance are shown collectively in Fig. 4.

The CO_2 purity always decreased with increasing γ , t_s and θ , whereas recovery decreased with decreasing γ , and increasing t_s and θ . The best performance based on purity was a CO_2 purity of 98.7% and a CO_2 recovery of 98.7%, with $\gamma = 0.02$, $t_s = 100$ s and $\theta = 5.8$ LSTP/hr/kg. Note the small γ was responsible for this very positive performance. The best result based on recovery was a CO_2 purity of 78.7% and a CO_2 recovery of 99.9%, with $\gamma = 0.50$, $t_s = 100$ s and

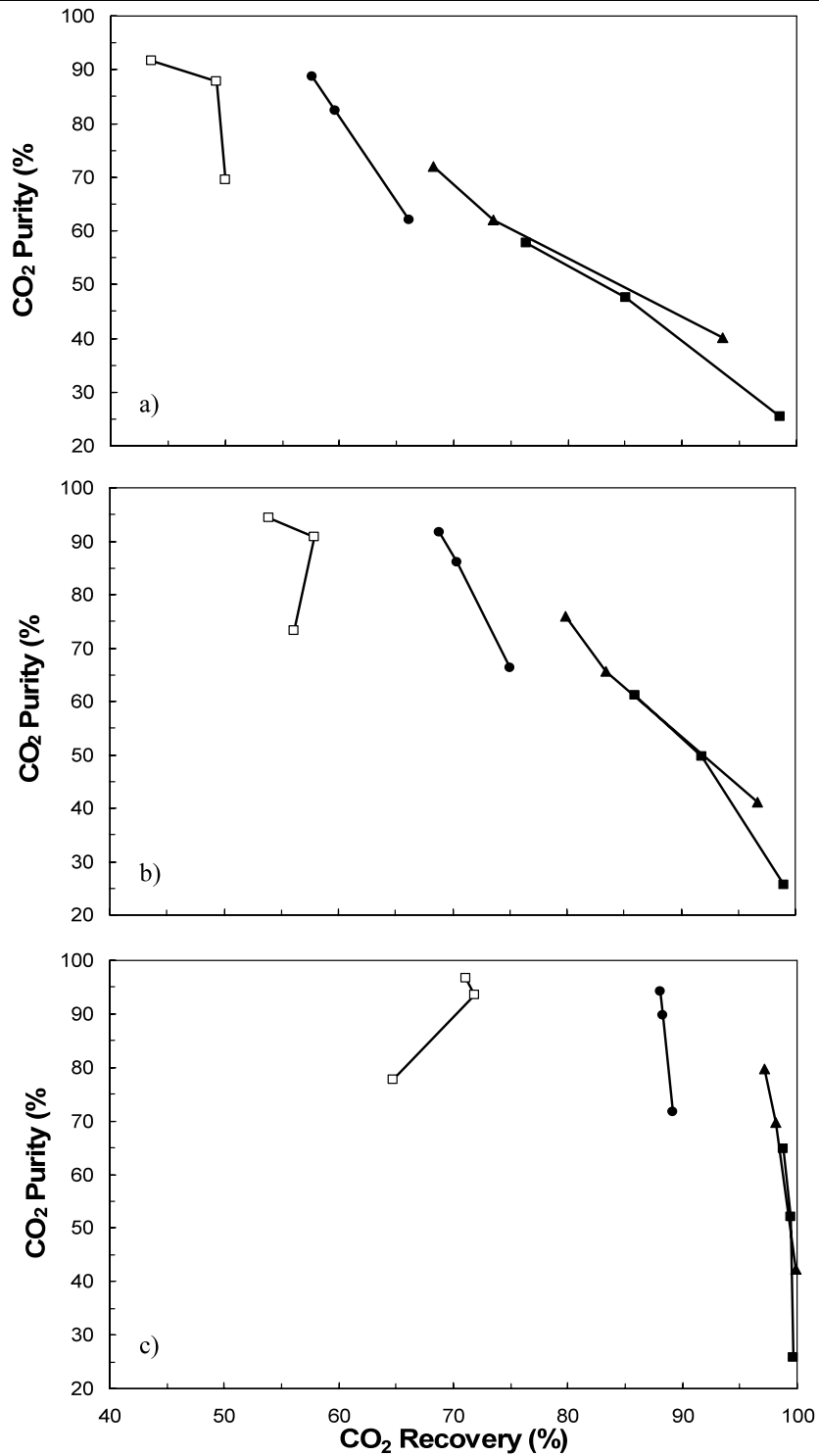
$\theta = 5.8$ LSTP/hr/kg. In this case, the larger γ improved the recovery, but only slightly and at the expense of decreasing the purity. Clearly, this HR PSA cycle is best suited for producing CO_2 at both high purities and high recoveries, but at relatively lower feed throughputs. These results are summarized and compared to all the other HR PSA cycles in Tables 2 and 3.

REC and F+R steps were also added to this 5-bed 5-step stripping PSA cycle with LR and HR from CnD, as shown in Figs. 1b and 1c, respectively. Simulations of these cycle variations were carried out with the same range of γ , t_s and θ . For the conditions studied and except at the lowest θ , if the results from these new cycle variations were plotted in Fig. 4, along with the curves for the same cycle without these steps, all the curves would essentially overlap each other (not shown). Hence, not only were the effects of γ , t_s and θ on the process performance approximately the same for such conditions, but also the effect of adding a REC or F+R step were surprisingly nil. The slight differences that did occur between these cycles at the lowest θ are shown in Fig. 5. Clearly, the addition of a REC or F+R step had a similar effect on the process performance with both of them lowering it compared to the cycle without them. The effect of these steps was expected to be much more pronounced. It was also expected to be favorable, not unfavorable.

5.2 Stripping PSA cycles with LR and HR from LR purge, with and without a REC or F+R step

The 5-bed 5-step stripping PSA cycle with LR and HR from LR purge consisted of five interconnected beds each undergoing in succession five cycle steps of equal duration, as

Fig. 6 Performance curves from the 5-bed 5-step stripping PSA cycle with LR and HR from LR purge (Fig. 2a) for $\gamma =$ (a) 0.02, (b) 0.10, and (c) 0.50. Each line corresponds to three runs with t_s increasing from right to left ($t_s = 100, 300,$ and 500 s). Symbols: filled squares— $\theta = 5.8$ ($Q_F = 0.5$); filled triangles— $\theta = 11.5$ ($Q_F = 1.0$); filled circles— $\theta = 34.6$ ($Q_F = 3.0$); empty squares— $\theta = 57.6$ ($Q_F = 5.0$). The performance curves from the corresponding stripping PSA cycle with LR, HR from CnD, and with REC or F+R were essentially the same (not shown)



shown in Fig. 2a. The only difference between this cycle and the one discussed in Fig. 1a was that the heavy product was recovered only during the CnD step and all the effluent from the LR step was recycled to the HR step. Just the opposite was done in the cycle in Fig. 1a. Again, the recycle ratio was equal to one ($R_R = 1.0$).

Thirty six different cases were simulated over the range of parameters listed in Table 2. Three light product purge to feed ratios (γ), three cycle step times (t_s), and four feed throughputs (θ) were investigated. The effects of γ , t_s , and θ on the process performance are shown collectively in Figs. 6a to 6c.

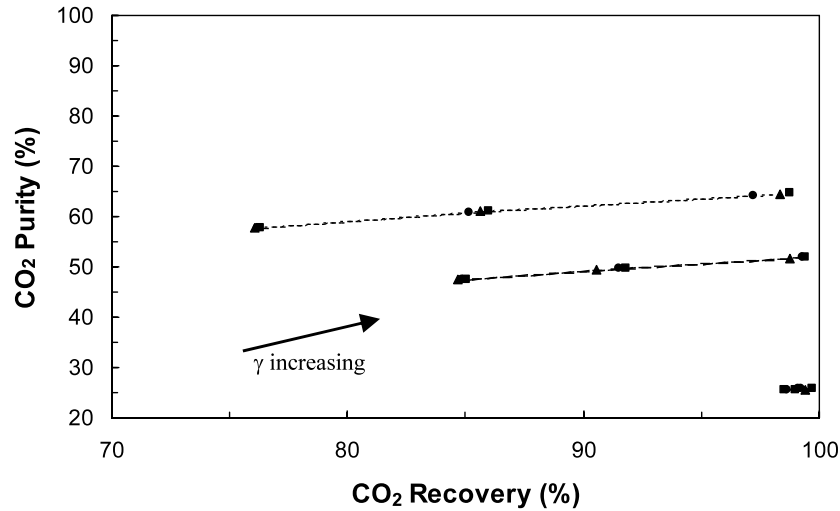


Fig. 7 Performance curves comparing the results from the three stripping PSA cycles with LR and HR from LR purge with and without REC or F+R steps and for $Q_F = 0.5$ L STP/min. Lines: solid (lowest curve)— $t_s = 100$ s; dashed (middle curve)— $t_s = 300$ s; dotted (upper curve)— $t_s = 500$ s. Symbols: squares—5-bed 5-step stripping PSA

cycle with LR and HR from LR purge ($\theta = 5.8$ L STP/hr/kg); triangles—6-bed 6-step stripping PSA cycle with LR, HR from LR purge and REC ($\theta = 4.8$ L STP/hr/kg); circles—5-bed 5-step stripping PSA cycle with LR, HR from LR purge and F+R ($\theta = 5.8$ L STP/hr/kg)

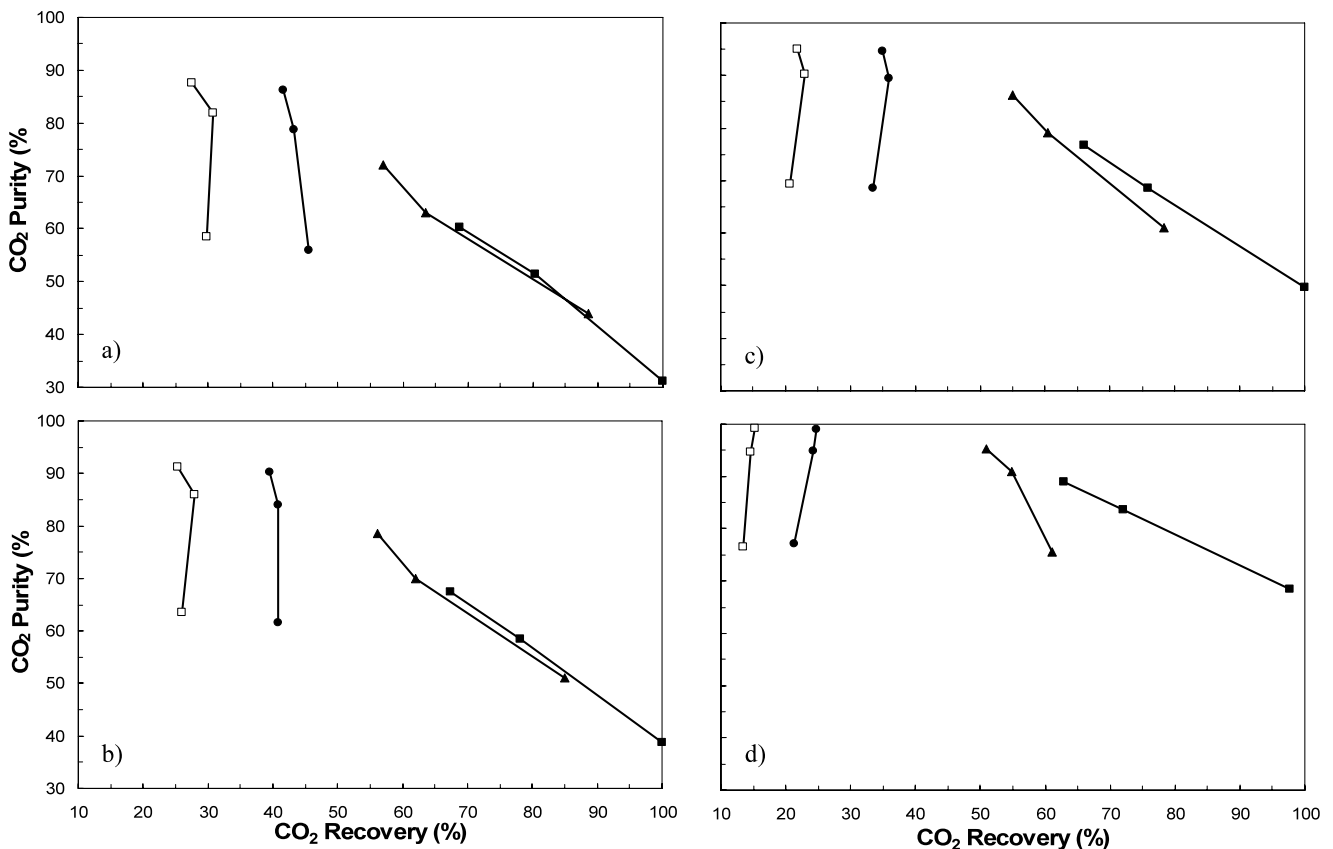
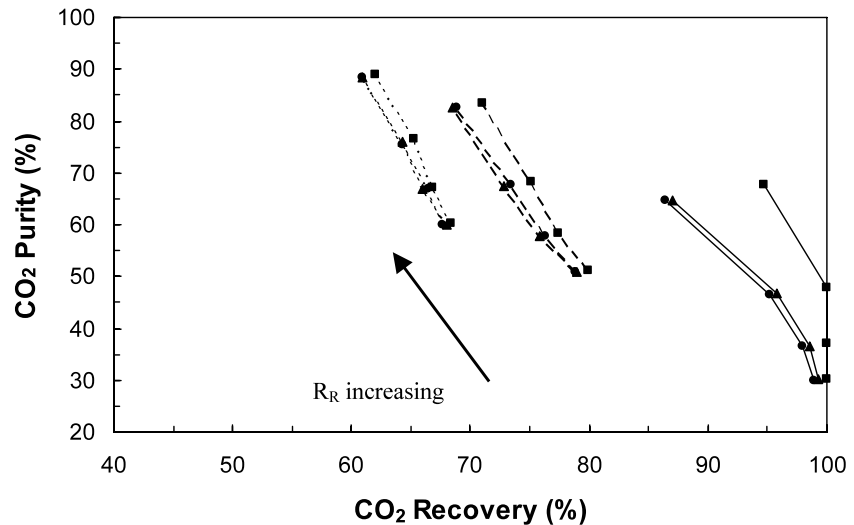


Fig. 8 Performance curves from the 4-bed 4-step stripping PSA cycle with HR from CnD (Fig. 3a) for $R_R =$ (a) 0.2, (b) 0.4, (c) 0.6 and (d) 0.8. Each line corresponds to three runs with t_s increasing from bottom to top ($t_s = 100, 300,$ and 500 s). Symbols: filled squares— $\theta = 7.2$ ($Q_F = 0.5$); filled triangles— $\theta = 14.4$ ($Q_F = 1.0$); filled circles— $\theta =$

28.8 ($Q_F = 2.0$); empty squares— $\theta = 43.2$ ($Q_F = 3.0$); empty triangles— $\theta = 57.6$ ($Q_F = 4.0$); empty circles— $\theta = 72.0$ L STP/hr/kg ($Q_F = 5.0$ L STP/min). The performance curves from the corresponding stripping PSA cycle with HR from CnD, and with REC or F+R were essentially the same (not shown)

Fig. 9 Performance curves comparing the results from the three stripping PSA cycles with HR from CnD with and without REC or F+R steps and for $Q_F = 0.5$ L STP/min. Lines: solid— $t_s = 100$ s; dashed— $t_s = 300$ s; dotted— $t_s = 500$ s. Symbols: squares—4-bed 4-step stripping PSA cycle with HR from CnD ($\theta = 7.2$ L STP/hr/kg); triangles—5-bed 5-step stripping PSA cycle with HR from CnD and REC ($\theta = 5.8$ L STP/hr/kg); circles—4-bed 4-step stripping PSA cycle with HR from CnD and F+R ($\theta = 7.2$ L STP/hr/kg)



The CO₂ purity increased with increasing γ , t_s and θ , and the CO₂ recovery decreased with decreasing γ and increasing θ . However, the effect of t_s on the CO₂ recovery was much more complex and depended on the values of both γ and θ , in some cases exhibiting a maximum as t_s increased. The best performance based on purity was a CO₂ purity of 96.6% and a CO₂ recovery of 71.1%, with $\gamma = 0.50$, $t_s = 500$ s and $\theta = 57.6$ L STP/hr/kg. The best performance based on recovery was a CO₂ purity of 42.2% and a CO₂ recovery of 99.9%, with $\gamma = 0.50$, $t_s = 100$ s and $\theta = 11.5$ L STP/hr/kg. Note that the larger γ produced the best performances for this cycle, a result that contrasted starkly with the previous cycle and indicated that the origin of the HR gas makes a significant difference. Clearly, this cycle is useful for producing CO₂ at both high purities and high feed throughputs, but at relatively lower recoveries compared to the HR PSA cycle with HR from CnD. These results are summarized and compared to all the other HR PSA cycles in Tables 2 and 3.

REC and F+R steps were also added to this 5-bed 5-step stripping PSA cycle with LR and HR from LR purge, as shown in Figs. 2b and 2c, respectively. Simulations of these cycle variations were carried out with the same range of γ , t_s and θ . Again, for all the conditions studied and except at the lowest θ , the addition of a REC or F+R step to this cycle had hardly any effect on its process performance. Hence, most of the results would essentially overlap each other if plotted in Fig. 6. The differences that did appear between these cycles at the lowest θ are shown in Fig. 7. The trends were the same as those in Fig. 5, but with even less pronounced but always unfavorable effects. These results were again very subtle and unexpected. Part II of this work provides an explanation (Mehrotra et al. 2007).

5.3 Stripping PSA cycles with HR from CnD, with and without a REC or F+R step

The 4-bed 4-step stripping PSA cycle with HR from CnD consisted of four interconnected beds each undergoing in succession four cycle steps of equal duration, as shown in Fig. 3a. The difference between this cycle and all the previous cycles was the elimination of the LR step. Hence, the heavy product was necessarily recovered during the CnD step, with a fraction of the effluent from this step being recycled to the HR step. This mode of operation was similar to that used in the previous studies of this cycle (Reynolds et al. 2006a, 2006b), wherein the recycle ratio R_R was varied from 0.2 to 0.8. The light product was still recovered during the F and HR steps.

Forty-eight cases were simulated over the range of parameters listed in Table 2. Four heavy product recycle ratios (R_R), three cycle step times (t_s), and four feed throughputs (θ) were investigated. The effects of R_R , t_s , and θ on the process performance are shown collectively in Figs. 8a to 8d.

The CO₂ purity always increased as R_R , t_s and θ increased. The CO₂ recovery always decreased with increasing R_R and θ . However, the effect of t_s on the CO₂ recovery was again much more complex and depended on the values of both R_R and θ , in some cases exhibiting a maximum as t_s increased. These trends are similar to the ones in Fig. 6, suggesting that the process performance depends strongly on the step from which the HR gas is obtained. The best performance based on purity was a CO₂ purity of 99.2% and a CO₂ recovery of 15.2%, with $R_R = 0.8$, $t_s = 500$ s and $\theta = 72.0$ L STP/hr/kg. The best performance based on recovery was a CO₂ purity of 37.1% and a CO₂ recovery of 100.0%, with $R_R = 0.4$, $t_s = 100$ s and $\theta = 7.2$ L STP/hr/kg. Compared to the two HR cycles with a LR step, the results of

this performance evaluation clearly revealed that the CO₂ recoveries of this cycle would always be much lower than the corresponding cycles with a LR step, no matter the process conditions. These results thus exposed the importance of the LR step to the process performance of these particular HR cycles for this application. These results are summarized and compared to all the other HR PSA cycles in Tables 2 and 3.

REC and F+R steps were also added to this 4-bed 4-step stripping PSA cycle with HR from CnD, as shown in Figs. 3b and 3c, respectively. Simulations of these cycle variations were carried out with the same range of R_R , t_s and θ . Again, for the conditions studied and except for the lowest θ , the addition of REC and F+R steps to this cycle did not have much effect on its process performance. Hence, most of results would essentially overlap each other if plotted in Fig. 8. The differences that did appear between these cycles at the lowest θ are shown in Fig. 9. The trends were the same as those in Figs. 5 and 7, but with some quite pronounced but always unfavorable effects, especially for the shortest cycle step time.

6 Conclusions

In this study nine different stripping PSA cycle configurations with HR were studied for concentrating CO₂ from stack and flue gas at high temperature using a K-promoted HTlc. The best performing cycle based on overall performance was the 5-bed 5-step stripping PSA cycle with LR and HR from CnD. The CO₂ purity was 98.7% and the CO₂ recovery was 98.7%, with $\gamma = 0.02$, $t_s = 100$ s and $\theta = 5.8$ L STP/hr/kg. This was a very exciting result, as the CO₂ purity and recovery were both very high. This very much improved performance was caused by the use of a very small γ ($\gamma = 0.02$). One of the drawbacks of this cycle configuration was the corresponding low feed throughput. Hence, this cycle was good at producing CO₂ at high purities and recoveries, but at lower feed throughputs. When adding either a REC or F+R step to this cycle, nearly identical performances were obtained, especially at the higher feed throughputs. At the lowest feed throughput studied, the differences that did manifest surprisingly were always unfavorable, with lower process performances resulting in both cases.

The next best performing cycle based on overall performance was the 5-bed 5-step stripping PSA cycle with LR and HR from LR purge. This cycle was able to produce a heavy product with a CO₂ purity of 96.5% and a CO₂ recovery of 71.1%, with $\gamma = 0.50$, $t_s = 500$ s and $\theta = 57.6$ L STP/hr/kg. Even though this cycle configuration did not provide as high of a CO₂ purity or CO₂ recovery as the other cycle with HR from CnD, it was very encouraging because the feed throughput was ten times higher, which

corresponded to ten times smaller columns. This much improved performance was caused by the use of a relatively larger γ ($\gamma = 0.5$). Hence, this cycle was good at producing CO₂ at high purities and feed throughputs, but at lower recoveries. The addition of a REC or F+R step to this cycle was similar to the previous case, with the process performance never improving.

The worst performing cycle based on recovery was the 4-bed 4-step stripping PSA cycle with HR from CnD. Although it was able to produce a heavy product with a high CO₂ purity of 99.2%, the CO₂ recovery was only 15.2%, with $R_R = 0.8$, $t_s = 500$ s and $\theta = 72.0$ L STP/hr/kg. This much diminished performance surprisingly was caused by the absence of a LR step in this HR cycle. Hence, this cycle was good at producing CO₂ at very low recoveries, but at high purities and feed throughputs. The addition of a REC or F+R step to this cycle was similar to the previous two cases.

Overall, this study revealed that changes in a HR cycle configuration that were initially thought to be only very slight turned out to have a marked effect on the process performance. For example, the biggest impact on the performance manifested when a LR step was added to the HR cycle, making it a dual reflux cycle. In turn, this made the performance depend very strongly on which step was used to produce the HR gas (or equivalently the heavy product gas). Significant and unexpected differences in the performances were obtained when the HR gas was obtained from the CnD step compared to the LR purge step, which meant that the heavy product gas was respectively produced from the LR purge and CnD steps. Conversely, changes in a HR cycle configuration that were initially thought to be very significant turned out to have only a minimal impact on its performance. For example, the addition of a REC or F+R step to a HR cycle was expected to improve the CO₂ recovery, but the impact turned out to be rather insignificant or even negative. These marked and sometimes subtle effects on the performance of a HR cycle were not expected and are explained in detail in Part II of this study.

Nomenclature

h	Overall heat transfer coefficient (kW/m ² /K)
ΔH_i	Isosteric heat of adsorption of component i (kJ/mol)
k_a	Adsorption mass transfer coefficient of CO ₂ (s ⁻¹)
k_d	Desorption mass transfer coefficient of CO ₂ (s ⁻¹)
L	Length of the bed (m)
P_H	High pressure (kPa)
P_L	Low pressure (kPa)
q_i	Loading of component i (mol/kg)

Q	Flow rate (L STP/min)
r_b	Radius of the bed (m)
R	CO ₂ recovery
R_R	Heavy product recycle ratio
t	Time (s)
t_s	Cycle step time (s)
T	Temperature (K)
u	Interstitial velocity (m/s)
y_i	Gas phase mole fraction of component i
$y_{\text{CO}_2, \text{HP}}$	Average gas phase mole fraction of CO ₂ in the heavy product
z	Axial coordinate in the column (m)

Greek letters

γ	Light product purge to feed ratio
θ	Feed throughput (L STP/hr/kg)

Subscripts

CnD	Countercurrent depressurization step
f	Feed
F	Feed step
F+R	Feed plus recycle step
HR	Heavy reflux step
i	Component i ($i = \text{CO}_2, \text{H}_2\text{O}$ or N_2)
LPP	Light product pressurization step
LR	Light reflux step
REC	Recovery step

Acknowledgements The authors gratefully acknowledge financial support provided in part by DOE Grant No. DE-FG26-03NT41799, and in part by MeadWestvaco and the newly formed Process Science and Technology Center, a joint collaboration between researchers at the University of Texas at Austin, the Texas A&M University, and the University of South Carolina.

References

- Chue, K.T., Kim, J.N., Yoo, Y.J., Cho, S.H., Yang, R.T.: Comparison of activated carbon and zeolite 13X for CO₂ recovery from flue gas by pressure swing adsorption. *Ind. Eng. Chem. Res.* **34**, 591–598 (1995)
- Ding, Y., Alpay, E.: Equilibria and kinetics of CO₂ adsorption on hydrotalcite adsorbent. *Chem. Eng. Sci.* **55**, 3461–3474 (2000)
- Ding, Y., Alpay, E.: High temperature recovery of CO₂ from flue gases using hydrotalcite adsorbent. *Trans Inst. Chem. Eng.* **79**, 45–51 (2001)
- Ebner, A.D., Ritter, J.A.: State-of-the-Art adsorption and membrane separation processes for carbon dioxide production in the chemical and petrochemical industries. *Adsorption* (2007, submitted)
- Ebner, A.D., Reynolds, S.P., Ritter, J.A.: Understanding the adsorption and desorption behavior of CO₂ on a K-promoted HTlc through non-equilibrium dynamic isotherms. *Ind. Eng. Chem. Res.* **45**, 6387–6392 (2006)
- Ebner, A.D., Reynolds, S.P., Ritter, J.A.: Non-equilibrium kinetic model that describes the reversible adsorption and desorption behavior of CO₂ in a K-promoted hydrotalcite-like compound. *Ind. Eng. Chem. Res.* **46**, 1737–1744 (2007)
- Hufton, J.R., Mayorga, S., Sicar, S.: Sorption-enhanced reaction process for hydrogen production. *AIChE J.* **45**, 248–256 (1999)
- Kikkindes, E.S., Yang, R.T., Cho, S.H.: Concentration and recovery of CO₂ from flue gas by pressure swing adsorption. *Ind. Eng. Chem. Res.* **32**, 2714–2720 (1993)
- Liu, Y., Holland, C.E., Ritter, J.A.: Solvent vapor recovery by pressure swing adsorption. I. Experimental study on the transient and periodic dynamics of the butane-activated carbon system. *Sep. Sci. Technol.* **33**, 2311–2334 (1998)
- Liu, Y., Holland, C.E., Ritter, J.A.: Solvent vapor recovery by pressure swing adsorption. III. Comparison of simulation with experiment for the butane-activated carbon system. *Sep. Sci. Technol.* **34**, 1545–1576 (1999)
- Mehrotra, A., Reynolds, S.P., Ebner, A.D., Ritter, J.A.: Heavy reflux PSA cycles for CO₂ recovery from flue gas: part II. Interpretation of trends. *Ind. Eng. Chem. Res.* (2008, submitted)
- Reynolds, S.P., Ebner, A.D., Ritter, J.A.: New pressure swing adsorption cycles for carbon dioxide sequestration. *Adsorption* **11**, 531–536 (2005)
- Reynolds, S.P., Ebner, A.D., Ritter, J.A.: Stripping PSA cycles for CO₂ recovery from flue gas at high temperature using a hydrotalcite-like adsorbent. *Ind. Eng. Chem. Res.* **45**, 4278–4294 (2006a)
- Reynolds, S.P., Ebner, A.D., Ritter, J.A.: Carbon dioxide capture from flue gas by PSA at high temperature using a K-promoted HTlc: effects of mass transfer on the process performance. *Environ. Prog.* **25**, 334–342 (2006b)
- Ruthven, D.M., Farooq, S., Knaebel, K.S.: *Pressure Swing Adsorption*. VCH, New York (1994)
- Soares, J.L., Moreira, R.F.P.M., Jose, H.J., Grande, C.A., Rodrigues, A.E.: Hydrotalcite materials for carbon dioxide adsorption at high temperatures: characterization and diffusivity measurements. *Sep. Sci. Technol.* **39**, 1989–2010 (2004)
- White, C.M., Strazisar, B.R., Granite, E.J., Hoffman, J.S., Pennline, H.W.: Separation and capture of CO₂ from large stationary sources and sequestration in geological formations—Coalbeds and deep saline. *J. Air Waste Manage. Assoc.* **53**, 645–715 (2003)